

Negatively charged trion in ZnSe single quantum wells with very low electron densities

O. Homburg, K. Sebald, P. Michler, and J. Gutowski

Institut für Festkörperphysik, Bereich Halbleiteroptik, Universität Bremen, P.O. Box 330440, D-28334 Bremen, Germany

H. Wenisch and D. Hommel

Institut für Festkörperphysik, Bereich Halbleiterepitaxie, Universität Bremen, P.O. Box 330440, D-28334 Bremen, Germany

(Received 23 March 2000)

The polarization- and excitation-intensity-dependent photoluminescence of the negatively charged trion is investigated for ZnSe single quantum wells embedded in ternary and quaternary barriers. The measurements were performed in magnetic fields up to 11.8 T perpendicular to the quantum well. The spin-singlet state of the trion is clearly identified. In contrast to GaAs quantum wells, the increase of the trion binding energy through the magnetic field is found to be negligible, which is explained by the relatively small spatial extent of the trionic wave function in wide-band-gap materials. For magnetic fields beyond 7 T a resonance becomes stabilized that is identified as excited trion spin-triplet state because of its anticorrelation with the trion spin-singlet state behavior for increasing excitation energy.

I. INTRODUCTION

Since the negatively charged trion (X^-) - consisting of an electron bound to an exciton - was first identified in CdTe/(Cd,Zn)Te quantum wells (QW's) quite recently in 1993 by Kheng *et al.*,¹ it was the subject of intense investigations, mainly concentrating on GaAs- and CdTe-based QW's.¹⁻⁹ Similarly, positively charged trions (X^+) - consisting of two holes and one electron - were studied.⁹⁻¹² In the following we concentrate on the negatively charged exciton. Since X^- consists of two identical fermions (electrons) the antiparallel orientation of their spins leads to a trion spin-singlet ground state (X_s^-) with zero total electron spin. The parallel electron spin orientation results in an excited spin-triplet state (X_t^-) with a total electron spin of one. Whereas X_t^- is unbound at zero magnetic field it becomes stabilized in strong fields.⁴ For GaAs-based QW's X_t^- was observed in a sub-meV distance from the $1s$ heavy-hole exciton resonance (X_{hh}). In spite of the small energy distances both lines were sharp and well separated due to the negligible localization in these ultrahigh-quality structures.^{3,4} With decreasing carrier density a strengthening of the X_t^- transition with respect to X_s^- was found and discussed.³

However, up to now, only very few studies on trions in ZnSe-based structures were performed,¹⁵⁻¹⁸ although the trion binding energy in ZnSe-based QW's is considerably increased compared to GaAs- and CdTe-based QW structures due to the larger exciton Rydberg energy of 20 meV in ZnSe bulk material. To our best knowledge, there is only one short report on first indications of a trion spin-triplet state in wide-band-gap materials like ZnSe.¹⁹ Therefore, we systematically investigate the formation of X_s^- and X_t^- in ZnSe/Zn(S,Se) and ZnSe/(Zn,Mg)(S,Se) single QW's (SQW's) by magneto-optical studies under stationary conditions. The samples are characterized by a very small inhomogeneous broadening of the X_{hh} resonance that results in a clear spectral separation of the trion and exciton resonances. Especially for the ZnSe/Zn(S,Se) QW's the electron and

trion concentrations are very low being of the order of 10^8-10^9 cm⁻² due to the small conduction-band offsets. Thus, insight into the trion formation in the very-low-density limit is obtained where X_t^- is expected to play an important role.

The paper is organized as follows. The sample structure, the experimental details, and results are given in Sec. II. The discussion follows in Sec. III. Some conclusions are drawn in Sec. IV.

II. EXPERIMENTAL SETUP AND RESULTS

All investigated ZnSe-based QW structures were pseudomorphically grown on GaAs substrates by molecular-beam epitaxy in an EPI 930 twin chamber system. First, we compare two 7-nm ZnSe/Zn(S,Se) SQW's with ternary-barrier widths of 100 nm. One of the samples is nominally undoped (in the following denoted by $S1$). The barriers of the other sample ($S2$) are intentionally n -doped to approximately 7×10^{17} cm⁻³ by Cl except for 50-nm-wide spacing layers adjacent to the undoped well. The total band offset between the barrier and the QW was deduced from photoluminescence (PL) measurements. For the nominally undoped sample it amounts to approximately 35 meV mainly occurring in the valence bands. The nominally doped sample yields slightly less electronic confinement with a total band offset of about 25 meV. Additionally, we investigate a nominally undoped 20-nm ZnSe/(Zn,Mg)(S,Se) SQW (sample $S3$). For this QW structure, the total band offset amounts to approximately 200 meV. A fraction of about 60% occurs in the valence bands in coincidence with values found for similar samples in the literature.^{20,21} The samples are characterized by means of reflection, polarization-dependent PL, and photoluminescence excitation (PLE) spectroscopy under continuous-wave laser excitation at cryogenic temperatures (1.5-2 K). For the magnetic-field-dependent measurements the samples were mounted in a 12-T magnet cryostat with the field perpendicular to the QW plane and parallel to the wave vectors of the incident and emitted light (Faraday con-

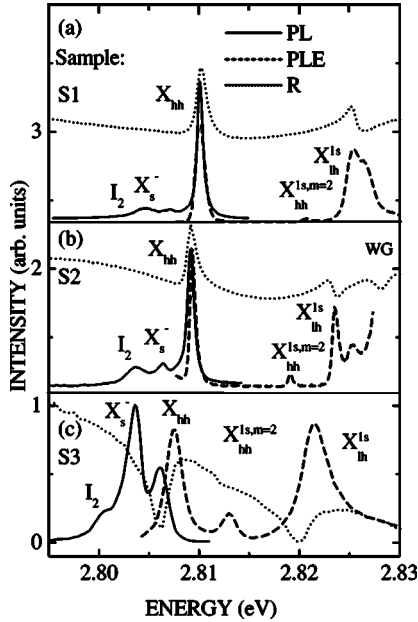


FIG. 1. PL (solid), reflectivity R (dotted), and PLE (dashed) spectra of samples $S1$ to $S3$, excited with a low excitation density of $P=1$ W/cm^2 at $T=2$ K.

figuration). The signal was dispersed by a monochromator and detected by a photomultiplier or an optical multichannel analyzer.

Reflectivity spectra, PL spectra for an excitation energy slightly above the barrier band edge, and PLE spectra for detection on the X_s^- trion line (see below) are recorded at $T=2$ K and a typical low excitation density of $P=1$ W/cm^2 (Fig. 1). The reflectivity spectra clearly show the $1s$ heavy-hole (X_{hh}) and the $1s$ light-hole exciton (X_{lh}) resonances, respectively. The PL spectra exhibit the X_{hh} and X_s^- transitions. The latter are identified by their characteristics in a magnetic field (see below). It is well known that trions can also be observed in nominally undoped structures due to the contamination with unintentional dopants.^{2,15} This is supported by the observation of a weak I_2 line that is typically 5 meV below the X_{hh} line for ZnSe and corresponds to a donor-bound exciton complex. For sample $S1$, the energy separation between the X_{hh} and X_s^- line amounts to 2.9 meV, which is an approximate estimate of the trion binding energy. Compared to sample $S1$, X_{hh} is found at a slightly lower energy for $S2$. The energy separation between the X_{hh} and X_s^- line exhibits a smaller value of 2.7 meV. These characteristics can be attributed to the slightly reduced electronic confinement in QW $S2$. In accordance with the barrier doping sample $S2$ exhibits a stronger X_s^- line intensity than sample $S1$, and a more pronounced I_2 line that indicates a stronger contamination of the QW with dopants. Compared to the samples $S1$ and $S2$, the intensity of the X_s^- line is much stronger for the nominally undoped QW $S3$. This is in accordance with the larger conduction-band offset of this sample resulting in a higher electron and thus trion density. For $S3$ the energy difference between the intensity maxima of the X_{hh} and X_s^- PL lines amounts to 2.5 meV. Since the well width of QW $S3$ is four times larger than the exciton Bohr radius of $a_B=4.8$ nm in ZnSe, this sample can be looked upon as being ‘‘bulklike’’ so that the binding en-

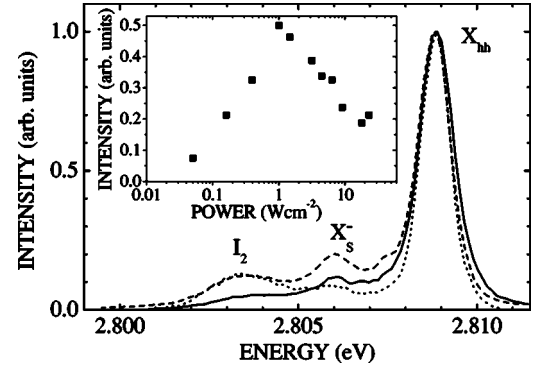


FIG. 2. Normalized PL spectra for sample $S2$ excited slightly above the barrier band edge ($E_{exc}=2.835$ eV) with different excitation intensities (solid line, $P=25$ W/cm^2 ; dashed line, $P=1$ W/cm^2 ; dotted line, $P=0.1$ W/cm^2) at 2 K. The spectra are normalized to the intensity maximum of the X_{hh} line. The inset shows the integrated intensity of the X_s^- line versus the excitation energy for this measurement.

ergy of the negatively charged trion can be assumed to amount roughly to 2.5 meV for bulk ZnSe.

The linewidth of the X_{hh} PL line amounts to 0.7, 0.9, and 1.9 meV for the samples $S1$, $S2$, and $S3$, respectively. It mainly originates from inhomogeneous broadening. Additionally, PLE measurements with a detection energy on the low-energy side of X_{hh} were performed. In the PLE spectra of the X_s^- lines, the $X_{hh}^{(1s,m=1)}$ resonance is observed together with the weaker $X_{hh}^{(1s,m=2)}$ quantized polariton mode (m mode number),¹³ pointing to the extremely good structural quality of the samples (see Refs. 13 and 14). The lowest X_{lh}^{1s} resonance is partly mixed with the X_{hh}^{2s} transition suggesting a relatively high strength. Additionally, for the samples $S1$ and $S2$ the onset of the barrier absorption is observed (partly not depicted in Fig. 1) at approximately 2.84 and 2.83 eV, respectively—in coincidence with the above stated difference of the total band offsets. The Stokes shift between the X_{hh} PL line and PLE resonance is less than 0.4 meV for the samples $S1$ and $S2$ and amounts to ≈ 1.3 meV for $S3$. Thus, localization effects are negligible particularly for the samples $S1$ and $S2$. Therefore, the following studies mainly concentrate on these QW’s.

In Fig. 2 the PL spectra at different excitation densities are exemplarily depicted for sample $S2$ when being excited slightly above the barrier band edge at 2 K. The spectra are normalized to the intensity maximum of the X_{hh} line. At the lowest excitation density ($P=0.1$ W/cm^2) the X_s^- line is very weak. With increasing excitation density the X_s^- line intensity at first exhibits a superlinear increase (see inset Fig. 2) and pass into a square-root-like increase. This indicates an increase of the excess electron density in the QW with the excitation density, however, followed by soon beginning saturation. This is discussed in Sec. III. At higher excitation densities ($P\approx 5$ W/cm^2)—corresponding to an electron-hole-pair density of about 10^9 cm^{-2} —the X_s^- line dramatically saturates. Obviously, this can be attributed to a limitation of the excess electron concentration n_e in the QW. Thus, a maximum n_e on the order of 1×10^9 cm^{-2} is deduced for sample $S2$. We note that the superlinear increase of the X_s^- line intensity contradicts its interpretation as a donor-bound-

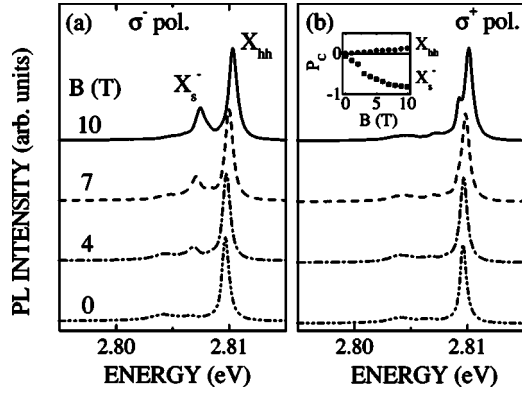


FIG. 3. PL spectra of sample *S1* excited via the barrier in dependence on the magnetic field for σ^- (a) and σ^+ (b) polarization at 2 K and a low excitation density ($P=0.1$ W/cm 2). Inset: Degree of polarization $P_c = (I_{\sigma^+} - I_{\sigma^-}) / (I_{\sigma^+} + I_{\sigma^-})$ for the X_{hh} and X_s^- lines in dependence on the magnetic field. $I_{\sigma^+}, I_{\sigma^-}$ denote the integrated intensities of the corresponding PL lines in σ^+ and σ^- polarization, respectively.

exciton transition. For such a complex, at first the ratio of its PL intensity with respect to X_{hh} is expected to stay nearly constant and then saturates with increasing excitation density—as observed for the I_2 line in Fig. 2.

For the nominally undoped sample *S1*, which is characterized by a slightly increased total band offset, a less pronounced superlinear increase of the X_s^- line intensity is observed at very low excitation densities. Additionally, the saturation occurs at a lower excitation density compared to sample *S2*. At $P=25$ W/cm 2 the X_s^- transition has already totally vanished. Conclusively, for this sample the QW excess electron concentration amounts to $n_e = 10^8 - 10^9$ cm $^{-2}$ only. For QW *S3* the X_s^- line intensity increases almost linearly at low excitation densities. At higher excitation densities (about 20 W/cm 2) it exhibits a clear sublinear increase being characteristic for saturation. These findings are in coincidence with a (nearly) constant excess electron concentration of several 10^9 cm $^{-2}$. For all samples the determined excess electron densities are quite low so that in a magnetic field the lowest Landau level with degeneracy $eB/h \approx 2.4 \times 10^{10} B / (\text{T cm}^2)$ can pick up all excess electrons already at a low field value of $B=1$ T.

In Fig. 3 the PL spectra of sample *S1* at 2 K obtained for excitation via the barrier at a low excitation density of $P=0.1$ W/cm 2 are depicted in dependence on the magnetic field B for σ^- (a) and σ^+ (b) polarized light. Most prominently, the σ^- polarized contribution (a) to the X_s^- line intensity strongly increases with magnetic field whereas it stays optically nearly inactive in σ^+ polarization (b). This polarization characteristic is consistent with the Zeeman splitting of X_s^- into a low-energy $m_j = -3/2$ and a high-energy $m_j = +3/2$ state due to the unpaired heavy-hole spin of $3/2$ in ZnSe [compare Fig. 5(b)]. Thus, the optical transition from the more strongly occupied $m_j = -3/2$ state to the electron ground state with $m_j = -1/2$ leads to the characteristic σ^- polarized X_s^- line. In the inset of Fig. 3(b) the degree of polarization $P_c = (I_{\sigma^+} - I_{\sigma^-}) / (I_{\sigma^+} + I_{\sigma^-})$ is depicted for the X_{hh} and X_s^- lines. $I_{\sigma^+}, I_{\sigma^-}$ denote the integrated intensities of the corresponding PL lines for σ^+ and σ^- polar-

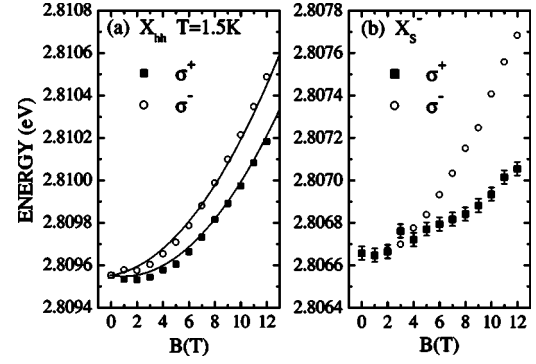


FIG. 4. X_{hh} (a) and X_s^- (b) Zeeman patterns of sample *S1* for σ^+ and σ^- polarization at 1.5 K. The solid and dashed lines (a) represent a fit of the X_{hh} energies in accordance with an excitonic Zeeman splitting and diamagnetic shift. The energies were extracted from PL measurements.

ization, respectively. Opposite to the strong σ^- dominance of the X_s^- line at high fields, a slightly σ^+ polarized X_{hh} line is observed, as expected for the recombination of neutral excitons (see, e.g., Ref. 2). The overall increase of X_s^- by a factor of about 4 governed by the increase of its σ^- component is discussed in detail in Sec. III.

In the case of σ^+ polarization a new emission feature on the low-energy shoulder of X_{hh} emerges for magnetic fields beyond 7 T. At $B=10$ T it is well-resolved separated from the X_{hh} maximum by $\Delta E=0.84$ meV. This line can be attributed to the trion spin-triplet state (X_t^-). Whereas X_t^- is unbound at $B=0$ T, it is expected to become stabilized in high magnetic fields and was first reported for GaAs QW's. 3,4 The correlation of the X_s^- and X_t^- lines in dependence on the excitation density is investigated in more detail below.

Figure 4 shows the Zeeman pattern of X_{hh} (a) and X_s^- (b) including identification of σ^+ [$E(\sigma^+)$] and σ^- [$E(\sigma^-)$] components for sample *S1* at $T=2$ K. The solid and dashed lines in Fig. 4(a) represent a fit to the data according to a Zeeman splitting of the heavy-hole exciton (in analogy to, e.g., Ref. 22)

$$\Delta E_{Zee} = E(\sigma^+) - E(\sigma^-) = g_{eff} \mu_B B, \quad (1)$$

with

$$g_{eff} := -(g_e + 3g_h) \quad (2)$$

and an excitonic diamagnetic shift

$$\Delta E_{Dia} = aB^2, \quad (3)$$

with the resulting fit function

$$E(B) = E(B=0) \pm g_{eff} \mu_B B + aB^2, \quad (4)$$

where g_{eff} , g_e , g_h , and μ_B denote the effective g factor, the electron and hole g factors, and the Bohr magneton, respectively. The constant a in Eq. (3) includes the spatial extension of the excitonic wave function that is not discussed in this paper. 23 With $g_{eff} = -0.33$ and $a = 5.7$ $\mu\text{eV/T}^2$ a very good agreement to the experimental data is obtained. Since the electron g factor is $g_e = +1.10$ (Ref. 24) for ZnSe the hole g factor can be calculated to $g_h = -0.26$ according to

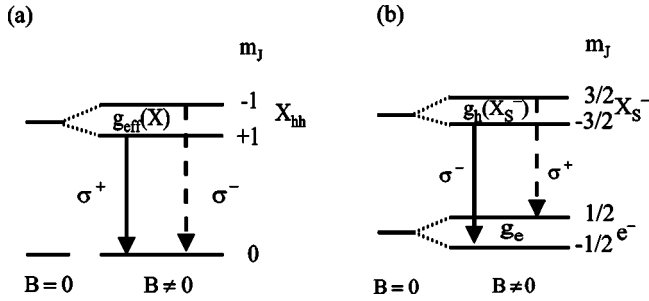


FIG. 5. Energy schemes and the optically allowed transitions of X_{hh} (a) and X_s^- (b) in a magnetic field. The solid arrows denote the strong polarization components. For the sake of clearness, only the spin-split lowest Landau levels are depicted for the trion X_s^- and the electron.

Eq. (2). Due to this calculation the heavy-hole state with $m_j = -3/2$ lies below $m_j = +3/2$ [compare Fig. 5(b)], this ordering being qualitatively consistent also with the above-discussed polarization degree of the X_s^- line. However, compared to X_{hh} a larger Zeeman splitting of X_s^- [Fig. 4(b)] is found. This can be explained by the larger spatial extent of the trionic wavefunction resulting in a different g_h , which may even change with the magnetic field.^{3,9} In fact, with increasing field, the X_s^- transition exhibits a decreasing g_{eff} from about zero at 0 T to -0.8 at 10 T as calculated according to Eq. (1). A similar decrease of the X_s^- Zeeman splitting was found by Glasberg *et al.* for GaAs QW's.⁹ Thus, in analogy to Ref. 9 the decrease of g_{eff} might be due to band mixing of the electron and hole wave functions with higher Landau levels and/or subbands.

However, with the exception of the larger Zeeman splitting compared to X_{hh} , the X_s^- resonance exhibits almost the same energy shift. This means that for this sample the stabilization of X_s^- in magnetic fields up to 10 T is negligible—in contrast to GaAs-based QW's where an increase of the trion binding energy of more than 60% was detected.^{3,9} We attribute this fact to the smaller spatial extent of the trionic wave function in ZnSe as implied by its larger binding energy $E_{X_s^-}^B \approx 2.9$ meV and smaller exciton Bohr radius $a_B = 4.8$ nm compared to GaAs ($E_{X_s^-}^B = 1-2$ meV, $a_B \approx 10$ nm). Thus, the effective electronic confinement induced by the magnetic field should be less for ZnSe—than for GaAs-based structures—in agreement with our experimental data.

In Fig. 5 the energy level diagrams of X_{hh} and X_s^- in a magnetic field are depicted with the separation of the energy levels due to the Zeeman splitting. The occupation thermalization of the energy levels at low temperature explains the dominance of the σ^+ (σ^-) polarized transition for the X_{hh} (X_s^-) in coincidence with the presented experimental data. To further support the presented trion energy scheme, PLE measurements at $B = 10$ T with a detection energy on the low-energy side of the X_s^- PL line were performed (not depicted). For the detection of the PL signal no polarizer was used. For σ^- polarized light, a strong excitation via the X_s^- resonance is observed. In contrast to that, no PLE signal can be detected under excitation with σ^+ polarized light—in co-

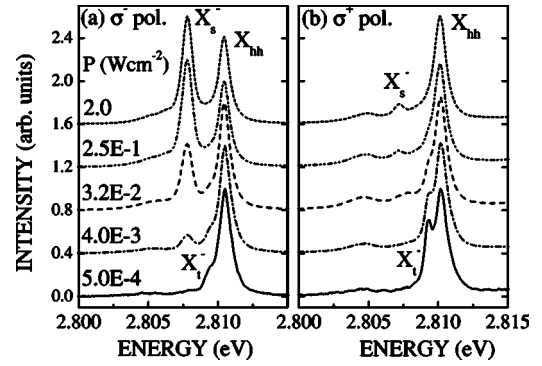


FIG. 6. PL spectra of sample $S2$ excited via the barrier in dependence on the excitation intensity for σ^- (a) and σ^+ (b) polarized light at $T = 1.5$ K.

incidence with a thermal occupation of the lowest electron energy level $m_j = -1/2$ only, as found also in other materials.^{1,2,15}

In Fig. 6 the PL spectra for σ^- (a) and σ^+ (b) polarized light are displayed in dependence on the excitation density at a magnetic field of $B = 11.8$ T and $T = 1.5$ K for sample $S2$ excited via the barrier. At the lowest excitation density, besides X_{hh} only the trionic triplet line X_t^- is observed for both cases (weak for σ^-). With increasing density the X_s^- line strongly evolves especially for σ^- polarized light, accompanied by a saturation of the X_t^- line indicating the correlation of these emission features. We note that the integrated intensity of the trionic PL (including the transitions X_s^- and X_t^-) increases first superlinearly with the excitation density—similar to the case of zero magnetic field (compare inset Fig. 2). In analogy to Ref. 3, the stronger intensity of the X_t^- line at very low carrier densities can be attributed to the larger spatial extent of the excited triplet state as implied by its small binding energy. This results in a more effective electron capture cross section of heavy-hole excitons thus converting into triplet-state trions at very low carrier densities.

Figure 7 shows the integrated intensities of the X_{hh} and X_s^- PL lines and their sum (I_{tot}) in dependence on the magnetic field for sample $S1$ (a) compared to sample $S3$ (b), both excited via their barriers with an excitation density of 1 W/cm² at 1.5 K. I_{tot} at $B = 0$ T is normalized to unity respectively, in the insets the corresponding PL spectra at magnetic fields of $B = 0$ T and $B = 10$ T are depicted. For this intermediate excitation density the X_t^- transition is already saturated. For sample $S1$ (a) the intensity of the X_s^- line stays constant at low magnetic fields up to 2 T. Beyond this field value, it shows a strong, nearly linear increase with magnetic field that is accompanied by a slight decrease of the X_{hh} PL line intensity. Thus, the increase of the total intensity of about 40% is mainly caused by the strengthening of the X_s^- transition. This is supported by the observation that at even higher excitation densities when the X_s^- line is already bleached no change of the total integrated intensity is found within an experimental error of about 10% (we note that with increasing magnetic field the alignment of the optics slightly changed which prevented the clear observation of smaller intensity changes). Sample $S2$ exhibits a similar strengthening of the X_s^- line as $S1$. However, QW $S3$ (b) shows a strongly deviating characteristic. The total integrated inten-

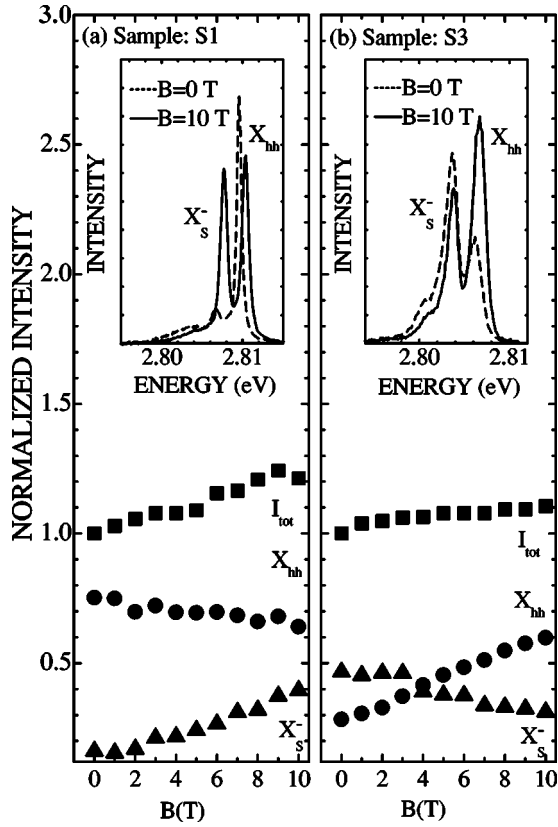


FIG. 7. Relative integrated intensities of the X_{hh} and X_s^- PL lines for sample S1 (a) and S3 (b) in dependence on the magnetic field at $T=1.5$ K. For both samples, the total integrated intensity (I_{tot}) at $B=0$ T is normalized to unity. The insets show the corresponding PL spectra at zero and the highest (10 T) applied magnetic fields.

sity exhibits only a slight increase with the magnetic field. The X_{hh} PL intensity increases strongly, almost linearly with B in the range between 0 and 10 T. In contrast the X_s^- line intensity stays nearly constant at magnetic fields up to 5 T and then exhibits a decrease of about 30%. In the following these characteristics are discussed in detail.

III. DISCUSSION

The experimental data give clear evidence that for all samples the X_s^- PL line is due to the electron-hole recombination from the negatively charged trion spin-singlet state. As a consequence of the small electronic confinement in the structures—either due to the low total band offsets (samples S1 and S2) or due to the large QW thickness (sample S3)—all QW's show small trion binding energies in the range of 2.5–2.9 meV. However, with varying total band offset and dopant concentration of the samples, the X_s^- line exhibits pronounced differences concerning its dependence on the excitation density (compare Fig. 2) or on a magnetic field (Fig. 7). A initial superlinear increase of the X_s^- line intensity at low excitation densities was found to be most pronounced for sample S2 excited via the barrier. We attribute this to an increase of the QW excess electron density with increasing excitation density. In thermodynamic equilibrium, i.e., without laser excitation, only a very low elec-

tron concentration accumulates in the QW S2 due to the small total band offset. Thus, at the lowest excitation densities only a very weak X_s^- line is observed (independent of the excitation energy). Under irradiation of light additional excess electrons and thus trions can be created. In the literature various mechanisms for the light-induced creation of excess electrons in different QW structures are discussed,^{25,26} which, however, are not applicable for the given excitation situation in our samples. Here, sample S2, as the first example, is characterized by a high donor dopant (bound electron) concentration in the barrier. Excitation of this sample via the barrier leads to a higher trion concentration in the QW than resonant excitation (via X_{hh} or X_{lh}). After excitation of the electron-hole pairs with the given low concentration, fast binding into excitons is followed by the onset of recombination. Either, donor scattering with excess energy, or even more, a two-electron process,²⁷ i.e., partial energy transfer from the recombining exciton to a donor electron, leads to an increase of the concentration of free excess electrons in the barrier conduction band [this process easily provides the Cl donor ionization energy of 26 meV (Ref. 27)]. After that, trions, on one hand, may already be formed in the barrier and then relax into the QW. However, considering the small trion binding energy, this process can practically be ruled out. On the other hand, in a more probable process, the neutral donor ionization by the above-mentioned processes is followed by unbound electron relaxation into the QW. Such a process should lead to an increase of the excess electron density with increasing excitation density which eventually results in the observed initial superlinear increase of the X_s^- line intensity.

In contrast to that, a fairly weakly superlinear increase of the X_s^- line intensity was observed for the nominally undoped sample S1 and a linear increase for S3, followed by early saturation. For these samples, no electron reservoir provided by a high amount of dopants is available, leading to a nearly constant excess electron density in the QW (at a constant magnetic field), which is fully used up for trion formation already at moderate excitation densities.

Another interesting feature which requires a thorough discussion is the dependence of the X_s^- and X_{hh} line intensities on the magnetic field. The intensity $I_{X(X^-)}(B)$ of the excitonic (trionic) radiative decay is given by

$$I_{X(X^-)}(B) = \frac{N_{X(X^-)}(B)}{\tau_{X(X^-)}(B)}, \quad (5)$$

with $N_{X(X^-)}(B)$, $\tau_{X(X^-)}(B)$ denoting the corresponding particle densities and the radiative decay times which depend on the magnetic field, respectively. Since the samples are characterized by very small inhomogeneous broadening we assume that the energy dependence of $\tau_{X(X^-)}$ is negligible. For sample S3 a decrease of the X_s^- line intensity with magnetic field was observed. A similar decrease of the X_s^- line intensity accompanied by an increase of the X_{hh} line intensity was also found in Ref. 28 for a GaAs QW with a large total band offset. However, this is not further commented upon in this paper. In analogy to Ref. 28 the decrease of the X_s^- line

intensity can be attributed to a decrease of the X_s^- coherence volume which is induced by the effective confinement caused by the magnetic field. This results in an increase of the radiative decay time. We note that the coherence volume usually has a spatial extent much larger than the exciton Bohr-orbit size. Thus, at high fields the coherence volume is limited by the magnetic length $l_B = [c\hbar/(eB)]^{1/2}$, which amounts to 8 nm at 10 T (compare: the exciton Bohr diameter is about 9.6 nm for ZnSe).

In contrast to S3, an increase of the X_s^- line intensity with increasing magnetic field was observed for the samples S1 and S2. Since for these QW's a similar magnetic-field-induced decrease of the coherence volume should hold, another mechanism has to overrule this effect. According to Eq. (5) we attribute the observed increase of the X_s^- line intensity to an increase of N_{X^-} with magnetic field. As we already pointed out above, in the QW's with low conduction-band offsets only very few electrons accumulate in the QW (at zero magnetic field). In addition to the confinement of the electrons, which is governed by the conduction-band offset (and the well width), the number of excess electrons in the QW is limited by their density of states at the band edge. Due to the low conduction-band offset it should be quite small, i.e., close to the bulk value. In a magnetic field the electron states split into Landau levels whose degeneracy increases proportionately to B . Thus, an increased amount of electrons proportional to B might accumulate in the QW leading to an almost linear increase of the X_s^- line intensity at elevated magnetic fields ($B \geq 2$ T).

However, time-resolved measurements are necessary to get more detailed information on the relaxation processes and kinetics of trions in these ZnSe-based QW structures.

IV. CONCLUSIONS

Trionic resonances have been identified in ZnSe quantum wells by means of excitation-intensity-dependent luminescence and polarization-dependent PL and PLE spectroscopy at moderate excitation densities. Trions are generated more effectively for excitation into the barrier than for resonant excitation into the quantum well. This points to the Cl donors in the barrier as being the source of the electrons. The magnetic-field-induced splitting and shift of the X_{hh} and the X_s^- resonances are in agreement with the expected energy level scheme. The effective g value of the trion was found to vary with magnetic field and to involve a g_h hole value deviating from that in the free exciton. The term ordering of the trion singlet state could be derived exhibiting a lower-lying $m_j = -3/2$ level. Due to the small spatial extension of the trion spin singlet state in ZnSe the increase of its binding energy with raising magnetic field is negligible. For σ^+ polarization at magnetic fields beyond 7 T, an emission feature emerges below the X_{hh} resonance, which was identified as trion spin-triplet X_t^- luminescence by means of the intensity anticorrelation of X_t^- and X_s^- for increasing excitation densities. The strong intensity of the X_t^- resonance relative to that of X_s^- at very low carrier densities is caused by the larger spatial extent of the triplet state leading to a more effective e^- capture.

In summary, a systematic investigation of trions in ZnSe QW's gave comprehensive insight into their internal structure and characteristic parameters.

ACKNOWLEDGMENTS

This work was supported by the Deutsche Forschungsgemeinschaft (Grant Nos. Gu 252/9-1 and Ho 1388/8).

-
- ¹K. Kheng, R. T. Cox, Y. Merle d'Aubigné, F. Bassani, K. Saminadayar, and S. Tatarenko, *Phys. Rev. Lett.* **71**, 1752 (1993).
 - ²K. Kheng, R. T. Cox, V. P. Kochereshko, K. Saminadayar, S. Tatarenko, Franck Bassani, and A. Franciosi, *Superlattices Microstruct.* **15**, 253 (1994).
 - ³A. J. Shields, M. Pepper, M. Y. Simmons, and D. A. Ritchie, *Phys. Rev. B* **52**, 7841 (1995).
 - ⁴D. M. Whittaker and A. J. Shields, *Phys. Rev. B* **56**, 15 185 (1997).
 - ⁵S. Lovisa, R. T. Cox, N. Magnea, and K. Saminadayar, *Phys. Rev. B* **56**, R12 787 (1997).
 - ⁶A. Manassen, E. Cohen, Arza Ron, E. Linder, and L. N. Pfeiffer, *Phys. Rev. B* **54**, 10 609 (1996).
 - ⁷G. Finkelstein, V. Umansky, I. Bar-Joseph, V. Ciulin, S. Haacke, J.-D. Ganière, and B. Deveaud, *Phys. Rev. B* **58**, 12 637 (1998).
 - ⁸M. Hayne, C. L. Jones, R. Bogaerts, C. Riva, A. Usher, F. M. Peeters, F. Herlach, V. V. Moshchalkov, and M. Henini, *Phys. Rev. B* **59**, 2927 (1998).
 - ⁹S. Glasberg, G. Finkelstein, H. Shtrikman, and I. Bar-Joseph, *Phys. Rev. B* **59**, R10 425 (1999).
 - ¹⁰A. J. Shields, J. L. Osborne, M. Y. Simmons, M. Pepper, and D. A. Ritchie, *Phys. Rev. B* **52**, R5523 (1995).
 - ¹¹D. Brinkmann, J. Kudrna, P. Gilliot, B. Hönerlage, A. Arnoult, J. Cibert, and S. Tatarenko, *Phys. Rev. B* **60**, 4474 (1999).
 - ¹²P. Gilliot, D. Brinkmann, J. Kudrna, O. Crégut, R. Lévy, A. Arnoult, J. Cibert, and S. Tatarenko, *Phys. Rev. B* **60**, 5797 (1999).
 - ¹³U. Neukirch, K. Wundke, J. Gutowski, and D. Hommel, *Phys. Status Solidi B* **196**, 473 (1996).
 - ¹⁴U. Neukirch, G. Bley, J. Gutowski, and D. Hommel, *Phys. Rev. B* **57**, 9208 (1998).
 - ¹⁵G. V. Astakhov, D. R. Yakovlev, V. P. Kochereshko, W. Ossau, J. Nürnberger, W. Faschinger, and G. Landwehr, *Phys. Rev. B* **60**, R8485 (1999).
 - ¹⁶W. Ossau, D. R. Yakovlev, U. Zehnder, G. V. Astakhov, A. V. Platonov, V. P. Kochereshko, J. Nürnberger, W. Faschinger, M. Keim, A. Waag, G. Landwehr, P. C. M. Christianen, J. C. Maan, N. A. Gippius, and S. G. Tikhodeev, *Physica B* **256-258**, 323 (1998).
 - ¹⁷S. Lovisa, R. T. Cox, T. Baron, M. Keim, A. Waag, and G. Landwehr, *Appl. Phys. Lett.* **73**, 656 (1998).
 - ¹⁸M. Godlewski, V. Y. Ivanov, J. P. Bergman, B. Monemar, K. Leonardi, M. Behringer, and D. Hommel, *Acta Phys. Pol.* **A 94**, 313 (1998).
 - ¹⁹V. Kutzer, H. Born, A. Hoffmann, A. Schätzer, and H. P. Wagner, in *Proceedings of the 24th International Conference on the Physics of Semiconductors, Jerusalem (Israel)*, edited by D. Gershoni (World Scientific, Singapore, 1999).

- ²⁰T. Miyajima, F. P. Logue, J. F. Donegan, J. Hegarty, H. Okuyama, A. Ishibashi, and Y. Mori, *Appl. Phys. Lett.* **66**, 180 (1995).
- ²¹P. Michler, M. F. Pereira Jr., O. Homburg, L. Nerger, J. Gutowski, H. Wensch, and D. Hommel, in *Proceedings SPIE 3625, Physics and Simulation of Optoelectronic Devices* (1999).
- ²²V. D. Kulakovskii, G. Bacher, R. Weigand, T. Kmmell, A. Forchel, E. Borovitskaya, K. Leonardi, and D. Hommel, *Phys. Rev. Lett.* **82**, 1780 (1999).
- ²³P. V. Giugno, A. L. Convertino, R. Rinaldi, R. Cingolani, J. Mas-sies, and M. Leroux, *Phys. Rev. B* **52**, 11 591 (1995).
- ²⁴J. Puls and F. Henneberger, *Phys. Status Solidi A* **164**, 499 (1997).
- ²⁵J. Siviniant, D. Scalbert, A. V. Kavokin, D. Coquillat, and J-P. Lascaray, *Phys. Rev. B* **59**, 1602 (1999).
- ²⁶H. P. Wagner, H.-P. Tranitz, and R. Schuster, *Phys. Rev. B* **60**, 15 542 (1999).
- ²⁷J. Gutowski, N. Presser, and G. Kudlek, *Phys. Status Solidi A* **120**, 11 (1990).
- ²⁸H. Okamura, D. Heiman, M. Sundaram, and A. C. Gossard, *Phys. Rev. B* **58**, R15 985 (1998).